VISUALIZED NDT FOR CONCRETE CRACKING BY SiGMA-AE AND SIBIE

Masayasu Ohtsu, Kentaro Ohno and Masanobu Tokai
Graduate School of Science and Technology, Kumamoto University, Japan

ABSTRACT

It is widely recognized that concrete structures are no longer maintenance-free. In order to inspect them for health monitoring and diagnosis, therefore, nondestructive testing (NDT) techniques are actively under development. For the practical use, visualized techniques are promising.

As one of NDT techniques, acoustic emission (AE) techniques have been extensively studied and practically applied to concrete structures. Currently, source kinematics of crack location, crack type and orientation can be quantitatively identified by SiGMA (simplified Green's functions for moment tensor analysis) procedure. Thus, AE source characteristics are visually studied in the process of diagonal-shear failure in reinforced concrete.

The impact-echo method has been developed for NDT of defects in concrete. Resonance frequencies of detected waves are applied to estimate the depth of defects in concrete. Because identifying particular peak frequencies responsible for the presence of defects is sometimes not easy, SIBIE (Stack Imaging of Spectral Amplitudes based on Impact-Echo) procedure has been developed. The procedure is applied to estimate the depth of a surface crack in concrete. It is demonstrated that the crack-depth is clearly visualized, even in the case that the crack is partially filled with water. In addition, an applicability to estimate the performance of repair work for a surface crack is studied.

KEYWORDS: Acoustic Emission, SiGMA, Impact Echo, SIBIE, Concrete Cracking

INTRODUCTION

Recently, concrete structures are no longer referred to as longer maintenance-free, because a number of structures are approaching to their service-life limit due to deterioration, aging and fatigue. As a result, diagnosis and health monitoring by nondestructive testing (NDT) techniques are in great demand and extensively investigated. In order to inspect existing structures for maintenance, visualized techniques are promising and to be developed for the practical use.

Crack nucleation and extension are readily detected and monitored by acoustic emission (AE). The generalized theory of AE has been established on the basis of elastodynamics [1]. It leaded to the moment tensor analysis of AE waves for source characterization [2]. Up to now, a simplified procedure has been developed as a SiGMA (Simplified Green's functions for Moment tensor Analysis) code, which is suitable for a PC-based processor and robust in computation [3]. Currently, results of the SiGMA analysis are visualized by introducing the virtual-reality modeling [4]. Here, cracking mechanisms of diagonal-shear failure in reinforced concrete are visually investigated by applying the SiGMA procedure.

In order to locate internal defects in concrete, the impact-echo method has been developed [5]. Resonance frequencies responsible for locations of defects (or voids) are extracted from frequency spectra of waves generated by driving an impact, and then the depths of defects are estimated from a relation between the travel distance and the wavelength of resonance. In order to circumvent the difficulty to identify peak frequencies in the conventional procedure, a new procedure has been developed as SIBIE (Stack Imaging of spectral amplitudes Based on the Impact-Echo) [6]. The procedure is successfully applied to imaging ungrouted tendon ducts in prestressed concrete members [7]. By applying the SIBIE procedure, the depth of a surface-opening crack in concrete is visually identified.

SiGMA ANALYSIS OF AE

Crack kinematics is theoretically represented by the moment tensor [3], which is defined by elastic constants and two vectors. The one vector is a crack-motion vector $\boldsymbol{b}$ and the other is a unit normal vector $\boldsymbol{n}$ to crack surface F. Mathematically, the moment tensor, M_{pq}, is formulated as,

$$M_{pq} = \int_F C_{pqkl}\, b(\boldsymbol{y}) l_k\, n_l\, dF = C_{pqkl} l_k n_l \left[\int_F b(\boldsymbol{y}) dF\right] = C_{pqkl} l_k n_l\, \Delta V. \quad (1)$$

Where C_{pqkl} is the tensor of elastic constants and $\boldsymbol{l}$ is the unit direction-vector of the crack-motion $\boldsymbol{b}$. ΔV represents the crack volume, which is obtained by integrating the crack-motion displacement $b(\boldsymbol{y})$ over the crack surface F, as given in eq. 1. It is noted that the moment tensor is defined by the product of the elastic constants [N/m^2] and the crack volume [m^3], leading to a moment [Nm] in mechanics as a physical unit. By the use of the moment tensor, AE wave $\boldsymbol{u}(\boldsymbol{x},t)$ is formulated,

$$u_k(\boldsymbol{x},t) = G_{kp,q}(\boldsymbol{x},\boldsymbol{y},t)\, M_{pq} * S(t). \quad (2)$$

Here $G_{ip,q}(\boldsymbol{x}, \boldsymbol{y}, t)$ means the spatial derivatives of Green's functions and $S(t)$ is kinetics of AE source and called the source-time function. Symbol * means the convolution integral.

In the SiGMA procedure, two parameters of the arrival time (P1) and the amplitude of the first motion (P2) are read from the waveform on a CRT screen. By applying the location procedure, crack location $\boldsymbol{y}$ is determined from the arrival-time differences at more than 5 sensors. Thus, distance R and its direction vector $\boldsymbol{r}$ are determined. Substituting the

amplitudes of the first motions at more than six channels into a simplified version of eq. 2, a series of algebraic equations are solved to determine components of the moment tensor. Since the SiGMA code requires only relative values of the moment tensor components, the relative calibration of the sensors is sufficient enough.

Classification of AE source into a particular crack-type is performed by the eigenvalue analysis of the moment tensor. It is assumed that dislocations of displacements at AE source consist of an opening motion (a tensile crack) and a lateral sliding motion (a shear crack). Setting the ratio of the maximum shear contribution as X, three eigenvalues for the shear crack become X, 0, -X. Likewise, the ratio of the maximum deviatoric tensile component is set as Y and the isotropic tensile as Z. Then, the eigenvalues of the moment tensor are normalized and decomposed as,

$$\begin{aligned} 1.0 &= X + Y + Z, \\ \text{the intermediate eigenvalue/the maximum eigenvalue} &= 0 - Y/2 + Z, \\ \text{the minimum eigenvalue/the maximum eigenvalue} &= -X - Y/2 + Z, \end{aligned} \qquad (3)$$

After solving eq. 3, AE sources, of which the shear ratios X are less than 40%, are classified into tensile cracks. The sources of X > 60% are classified as shear cracks. In between 40% and 60%, cracks are referred to as mixed mode. In the eigenvalue analysis, three eigenvectors are also determined, and then the two vectors ***l*** and ***n***, which are interchangeable, are recovered. The software is currently built-in in an AE equipment as shown in Figure 1.

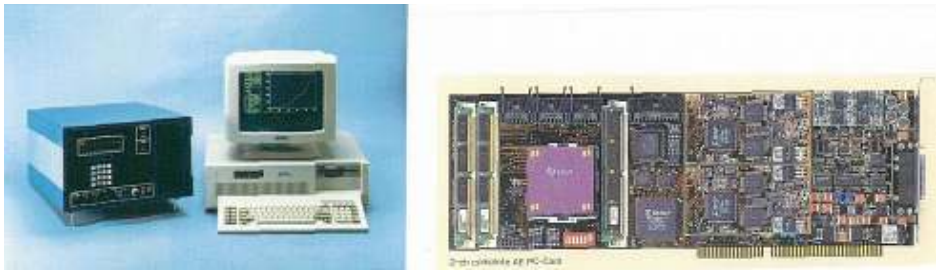

Fig. 1 AE equipment with SiGMA software.

SIBIE PROCEDURE

In the impact-echo method, an impact is applied to the surface of concrete, and a generated elastic wave is detected. Then a peak frequency is identified from a frequency spectrum after FFT (Fast Fourier Transform) analysis of the detected wave. An impact of good power and higher frequency components is desirable, although conventionally a steel-ball drop is employed. Since high frequency components are able to be generated by the drop of a small ball with a short contact-time, a high-frequency impact is often less powerful. Consequently, a portable device to drive an impact is developed, and is shown in Fig. 2. An aluminum bullet of 8 mm diameter is shot through a tube of 10 mm inner-diameter by driving compressed air of 0.05 MPa. It is demonstrated that the use of this system could provide the frequency components over 40 kHz with the amplitudes high enough [6]. In addition, it is found that the frequency range of the conventional impact-echo device is limited to 30 kHz. Elastic waves due to the impact were detected by an accelerometer, of which the frequency range was found to cover approximately up to 55 kHz.

Of a detected wave, its frequency spectrum normally contains many peak frequencies. So, it is complicated and sometimes uncertain to correctly pick up the relevant peaks to defects. An imaging procedure has been developed [6], which is applied to a result of the Fourier spectrum. In the procedure, at the reflection point at a cross-section in Fig. 3, the dominated resonance components are mathematically calculated from,

$$f_1 = v_P/r_1, \text{ and } f_2 = v_P/R \quad (4)$$

Fig. 2 Aluminum bullet and portable impactor.

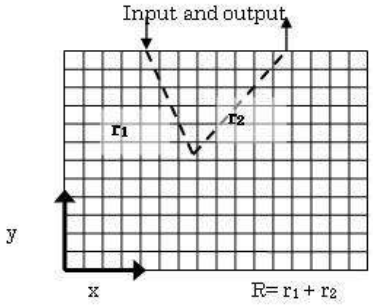

Fig. 3 Mesh division and travel path.

Here, the cross-section is divided into rectangular elements. At the center of each element, the distance R from the incident to the reflected path is calculated. Then, two resonance frequencies are computed from eq. 4, where v_P is the velocity of P wave. The spectral amplitudes corresponding to these resonance frequencies are stacked at the element. Thus, the intensity of reflections at each element is relatively estimated as a stack image.

RESULTS AND DISCUSSION

(1) Crack Kinematics of Diagonal Shear Failure

In order to generate diagonal-shear failure in a shear span of a reinforced concrete (RC) beam, a beam of dimensions 150 mm × 250 mm × 2000 mm with 400mm shear span was designed as the ratio of a shear span to an effective depth was set to 1.97. The specimen is illustrated in Fig. 4 along with arrangement of reinforcement. Concerning mechanical properties of hardened concrete, the compressive strength was 29. 7 MPa and the velocity of P wave was 4320 m/s. To monitor diagonal-shear failure in the RC beam with AE sensors, stirrups were arranged only in one half portion of the specimen. 8 sensors were arranged in another shear span (a right portion in Fig. 4) without the stir-up reinforcement. The sensor arrangement is shown in Fig. 5. Locations of AE sensors were determined from numerical experiments [8].

AE monitoring was conducted under two-point loading in the bending test of the beam. AE signals were detected by AE sensors of 150 kHz resonance (R15, PAC) and processed (DiSP, PAC). The frequency range was from 15 kHz to 300 kHz. The sampling frequency for recording waveforms was 1 MHz with 2048 words. AE hits were amplified with 40 dB gain in a pre-amplifier and 20 dB gain in a main amplifier. The threshold level for detection was set to 42 dB.

A relation between loads and total AE hits observed at all channels during the test is shown in Fig. 6. The ultimate load of the RC beam was 96.1 kN, when the diagonal-shear

failure was observed. Here, a loading process is divided into three stages. Stage 1 is the period from the beginning to 53 min. elapsed, where the number of AE hits is a few and no bending cracks were observed. In Stage 2 from 53 min. to 68 min., AE hits were actively observed, and bending cracks were visually found at the bottom of the center span. The number of AE hits increased further after short-term low activity. Diagonal-shear failure was observed during the final Stage 3.

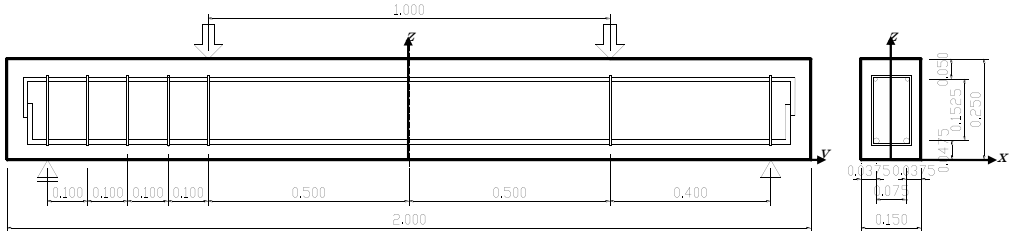

Fig. 4 Sketch of RC specimen (unit:m)

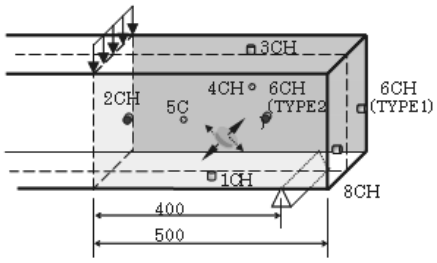

(mm)

Fig. 5 AE sensor array.

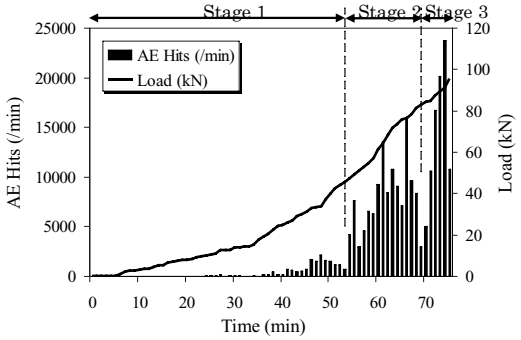

Fig. 6 AE generating behavior under bending

From a waveform set of 347 AE events detected, locations of sources were determined by reading the arrival times of P-waves. On 187 events out of 347 events, however, the convergence of solutions could not reach the criterion. Therefore locations of 160 events were determined. Then, moment tensor components were determined by the SiGMA analysis. Results are illustrated in Fig. 7 with three crack models.

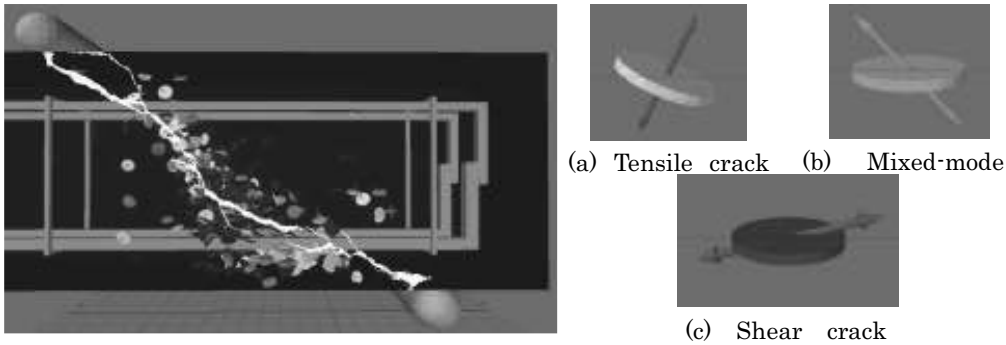

(a) Tensile crack (b) Mixed-mode

(c) Shear crack

Fig. 7 Crack kinematics during the diagonal-shear failure in RC beam.

All AE sources are observed close to the plane of diagonal shear failure. Directions of crack opening are almost perpendicular, and shear cracks are parallel to the diagonal-shear failure surface. This demonstrates an applicability of the SiGMA procedure to visually study failure process inside concrete.

Although AE events were actively detected at Stage 2, the final diagonal-shear failure was observed eventually at Stage 3. Crack kinematics observed only at Stage 2 are shown in Fig. 8. It is interesting that three types of cracks are mixed up, but they clearly distribute around the final failure in Fig. 7. This implies that the fracture process zone was created before generating the diagonal-shear failure planes. It suggests that earlier warning of the shear failure, which is always suddenly observed, might be possible by AE monitoring.

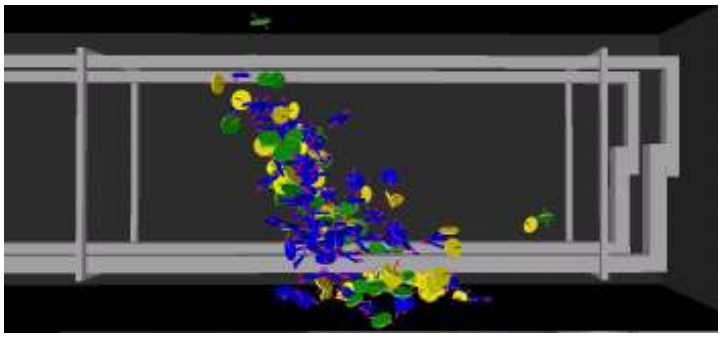

Fig. 8 Crack kinematics at Stage 2.

(2) Depth of Surface Crack

Experiments were carried out in a laboratory on a concrete block with a surface-crack. As shown in Fig. 9, an artificial surface-crack of 0.5 mm width is located in the middle of the top surface, which was made by placing a metal plate when casting concrete. The plate was removed one day after. The specimen of dimensions 400mm x 250mm x 300mm was made with a crack of 100mm depth. Test was conducted when the crack was empty (open) and after the crack was filled with water up to 80% depth.

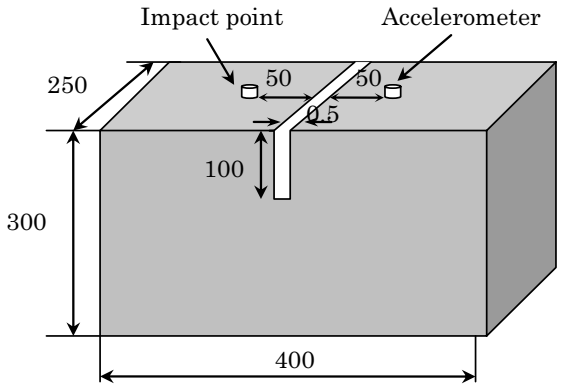

(mm)

Fig. 9 Specimen with a surface crack.

In the test, shooting an aluminum bullet at the impact point, elastic waves were detected at the detection point across the crack by the accelerometer. Sampling time was 4 μsec and the number of digitized data for each waveform was 2048. The case of 100 mm distance between the impact point and the detection is discussed.

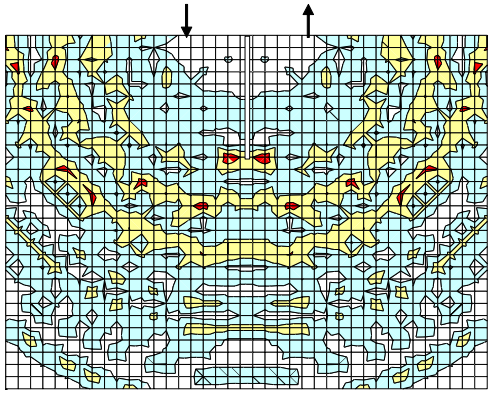

Fig. 10 SIBIE analysis in an open crack.

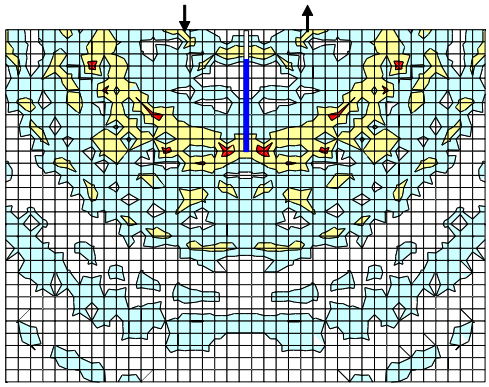

Fig. 11 SIBIE analysis in a water-filled crack.

In Fig. 10, a result of the SIBIE analysis in an open crack is given. The crack is indicated as white zone. The mesh elements are arranged at 10-mm pitch evenly. In the figures, dark color regions indicate the high intense regions due to the resonance of diffraction. Arrows show locations of the impact and the detection. A high-intense diffraction zones clearly exist in the vicinity of the crack tip. Thus, it is demonstrated that the depth of a surface crack is visually identified by the SIBIE procedure.

In the case of a water-filled crack, it is known that the crack-depths might be referred to as shallow in the ultrasonic test, due to reflection at water surface. A result of the SIBIE analysis is shown in Fig. 11. The surface crack is indicated as a white zone and water part of the crack is indicated as a dark zone. It is found that diffraction of dark color regions are particularly observed around the crack tip, and no intense zone is observed around the water surface. This demonstrates that the SIBIE procedure is applicable to estimate the depth of surface-crack filled with water.

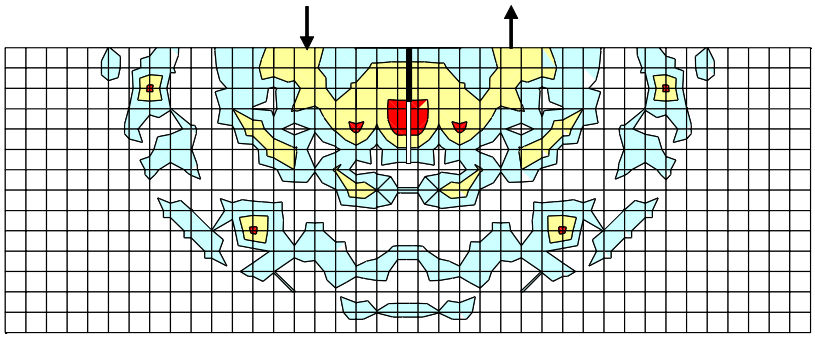

Fig. 12 SIBIE analysis in an improperly repaired crack.

In addition, the case of an improperly repaired crack was examined. The open crack was repaired, as only the upper-half depth was filled with cement grout. Then, the SIBIE procedure was applied. Results are given in Fig. 12. It is found that at the depth of the ungrouted crack, high intense areas are visually observed. This demonstrates that grouting performance of repair work for the surface crack could be estimated by the SIBIE procedure.

CONCLUSIONS

For visualized NDT techniques, the SiGMA analysis of AE and the SIBIE procedure of impact-echo are investigated. Results obtained are summarized, as follows:

(1) Kinematics of cracks can be quantitatively analyzed by applying the SiGMA code, and can be visually displayed for identifying failure process. In the bending test of a reinforced concrete beam, diagonal-shear failure process was clarified. According to the SiGMA analysis, opening directions of tensile cracks were almost perpendicular to the failure plane, and motions of shear cracks were parallel to the final crack surface. It is noted that many AE events, which were located around the diagonal-shear failure, were actively observed at Stage 2 prior to the nucleation of the final failure.

(2) In the ultrasonic test, it is often difficult to identify first motions of arrival waves for the surface-crack measurement. By applying the SIBIE procedure, the cases of an open crack and a water-filled crack were tested. In all the cases, the depths of surface-opening cracks can be visually identified. In the case of an improperly grouted crack, an un-grouted part of the crack was also successfully visualized.

REFERENCES

[1] Ohtsu, M. and Ono, K. (1984),"A Generalized Theory of Acoustic Emission and Green's Functions in a Half Space," *Journal of AE*, Vol. 3, No. 1, 124-133.

[2] Kim, K. Y. and Sachse, W. (1984),"Characterization of AE Signals from Indentation Cracks in Glass," *Progress in Acoustic Emission II*, JSNDI, 163-172.

[3] Ohtsu, M.(1991),"Simplified Moment Tensor Analysis and Unified Decomposition of Acoustic Emission Source : Application to In Situ Hydrofracturing Test," *Journal of Geophysical Research*, Vol. 96, No. B4, 6211-6221.

[4] M. Ohtsu and M. Shigeihsi,"Virtual Reality Presentation of Moment Tensor Analysis by SiGMA," *J. Korean Soc. for NDT,* Vol. 23, No. 3, pp. 189-1999, 2003.

[5] Sansalone, M. J. and Streett, W. B.(1997), *Impact-Echo*, Bullbrier Press, Ithaca, N. Y..

[6] Ohtsu, M. and Watanabe, T.(2002),"Stack Imaging of Spectral Amplitudes based on Impact-Echo for Flaw Detection," *NDT & E International*, Vol. 35, No. 3, 189-196.

[7] Ata, N., Mihara, S. and Ohtsu, M.(2007),"Imaging of Ungrouted Tendon Ducts in Prestressed Concrete by Improved SIBIE," *NDT & E International*, Vol. 40, No. 3, 258-264.

[8] Ohno, K., Shimozono, S. and Ohtsu, M.(2007),"Cracking Mechanisms of Diagonal-Shear Failure monitored and identified by AE-SiGMA Analysis," *Fracture Mechanics of Concrete and Concrete Structures*, Taylor & Francis, London, Vol. 2, 991-998.